



# Moisture sources of heavy precipitation in Central Europe in synoptic situations with Vb-cyclones

Amelie Krug<sup>1</sup> · Franziska Aemisegger<sup>2</sup> · Michael Sprenger<sup>2</sup> · Bodo Ahrens<sup>1</sup>

Received: 18 December 2020 / Accepted: 10 March 2022 / Published online: 25 April 2022  
© The Author(s) 2022

## Abstract

During the past century, several extreme summer floods in Central Europe were associated with so-called Vb-cyclones propagating from the Mediterranean Sea north-eastward to Central Europe. The processes intensifying the precipitation in synoptic situations with Vb-cyclones in the Danube, Elbe, and Odra catchments are only partially understood. Our study aims to investigate these processes with Lagrangian moisture-source diagnostics for 16 selected Vb-events. Moreover, we analyse the characteristics of typical moisture source regions during 1107 Vb-events from 1901 to 2010 based on ERA-20C reanalysis dynamically downscaled with COSMO-CLM+NEMO. We observe moisture contributions by various source regions highlighting the complex dynamical interplay of different air masses leading to moisture convergence in synoptic situations with Vb-cyclones. Overall, up to 80% of the precipitation originates from the European continent, indicating the importance of continental moisture recycling, especially within the respective river catchment. Other major moisture uptake regions are the North Sea, the Baltic Sea, the North Atlantic, and for a few events the Black Sea. Remarkably, anomalies in these oceanic source regions show no connection to precipitation amounts in synoptic situations with Vb-cyclones. In contrast, the Vb-cyclones with the highest precipitation are associated with anomalously high evaporation in the Mediterranean Sea, even though the Mediterranean Sea is only a minor moisture source region on average. Interestingly, the evaporation anomalies are not connected with sea-surface temperature but with wind-speed anomalies (Spearman's rank correlation coefficient  $R \approx 0.7$ , significant with  $p < 0.01$ ) indicating mainly dynamically driven evaporation. The particular role of the Mediterranean Sea hints towards possible importance of Mediterranean moisture for the early-stage intensification of Vb-cyclones and the pre-moistening of the continental uptake regions upstream of the target catchments.

**Keywords** Vb-cyclones · Heavy precipitation events · Danube · Elbe · Odra · Marginal seas · Twentieth century reanalysis

## 1 Introduction

River floods are the most common and devastating natural hazard in Europe. Floods differ not only according to the spatial extent, temporal duration, and peak discharges, but also in terms of the hydroclimatic and hydrological causes (Tarasova et al. 2019). In this study, we focus on precipitation occurring in weather situations associated with so-called Vb-cyclones that can trigger widespread floods in Central Europe, especially during the summer season (e.g.,

Blöschl et al. 2013). These extratropical cyclones are defined by their pathway from the western Mediterranean Sea north-eastward over northern Italy along the eastern fringe of the Alps to Central Europe (van Bebber 1891). Many devastating summer floods in the Central European macro-scale catchments of the Odra, Elbe, and Danube rivers were associated with that cyclone pathway.

The classification of this special cyclone pathway goes back to van Bebber (1891). Vb-cyclones occur rarely with about 2–10 events per year on average (Hofstätter and Chimani 2012; Messmer et al. 2015; Hofstätter and Blöschl 2019). Nonetheless, they are of high relevance for extreme precipitation events and floods in central and eastern Europe. Messmer et al. (2015) concluded that 15% of the extreme precipitation (99th percentile) over Central Europe and the northern Alpine region are associated with Vb-cyclones. About 45% of the Vb-cyclones are linked with heavy precipitation (95th percentile) in the Czech Republic and eastern Austria

✉ Amelie Krug  
krug@iau.uni-frankfurt.de

<sup>1</sup> Institute for Atmospheric and Environmental Science, Goethe University Frankfurt, Frankfurt am Main, Germany

<sup>2</sup> Institute for Atmospheric and Climate Science, ETH Zürich, Zurich, Switzerland

(Hofstätter et al. 2018), and about 40% of Vb-cyclones correlate with heavy precipitation (95th percentile) in the Elbe catchment, especially during April and May (Nissen et al. 2013). In particular, Vb-cyclones with a distinct cutoff low in upper levels are linked to heavy precipitation (Messmer et al. 2015; Hofstätter et al. 2018; Mittermeier et al. 2019).

Vb-cyclones occur throughout the year with a peak frequency in spring (Hofstätter and Chimani 2012; Messmer et al. 2015). Hofstätter et al. (2016) analysed the seasonal dependence of cyclone intensity for various pathways including the Vb-type. Measures for the cyclone intensity are, for example, the minimum core pressure or the maximum relative vorticity. The median intensity of Vb-cyclone shows no distinct seasonal cycle. Vb-cyclones are among the strongest cyclones in Europe throughout the year, also with respect to cyclone precipitation (Hofstätter et al. 2016, 2018). During winter, some Vb-cyclones cause heavy snowstorms in Central Europe. An example is the Vb-cyclone in January 2010 (Nissen et al. 2013).

Vb-cyclones are associated with extreme and widespread floods in Central Europe mainly during the summer half-year (e.g., Blöschl et al. 2013; Hofstätter et al. 2016). Closer inspection reveals that the Vb-cyclone intensity is highly variable during the summer season in terms of the relative vorticity and often surpasses the intensity of Atlantic cyclones in winter that are related to winter storms in Europe (Hofstätter et al. 2016). During winter, the main Vb-cyclogenetic processes are the dynamic coupling between the upper-level and the low-level orographic flow (e.g., in the Alpine region), as well as low-level baroclinicity (Aebischer and Schär 1998; Trigo et al. 2002; Hofstätter et al. 2016). During summer, however, an essential additional ingredient for intense Vb-events are high equivalent potential temperatures and latent heat release in lower atmospheric levels over northern Italy on the lee-side of the Alps (Aebischer and Schär 1998). This is supported by the sensitivity studies of Volosciuk et al. (2016) and Messmer et al. (2017) that showed an intensification of Vb-cyclone precipitation in Central Europe with increasing sea surface temperatures (SSTs) of the Mediterranean Sea. Furthermore, higher temperatures during summer increase the total water content (Hofstätter and Chimani 2012) and thus moisture transport in the atmosphere, which in turn decreases the atmospheric stability and favours upward motion and precipitation (Messmer et al. 2017). Due to the meridionally curved cyclone path, precipitation is then initiated especially along west-east oriented central European barriers like the Alps and Ore mountains (Grams et al. 2014). Note that Messmer et al. (2017) found conversely a decrease of precipitation over the north-eastern flanks of the Alps for higher SSTs over the Mediterranean. This can be explained by an increase in precipitation along the eastern Adriatic coasts and thus decreased moisture flux north-eastward of the Alps.

However, not only the Mediterranean Sea is an evaporative moisture source during Vb-events. Besides the Mediterranean Sea, also the North Atlantic and Black Sea are relevant moisture sources, for example, during the August 2002 flood (James et al. 2004; Sodemann et al. 2009; Gangoiti et al. 2011b). In addition, moisture recycling over the European continent contributed to the heavy rainfall, especially towards the end of the event (James et al. 2004; Gangoiti et al. 2011a, 2015). In August 2005 (Winschall 2013), May 2010 (Winschall et al. 2014), and May/June 2013 (Grams et al. 2014; Kelemen et al. 2016), moisture recycling over the European continent and the North Atlantic dominated, while the Mediterranean Sea only weakly contributed to the heavy rainfall. In contrast to the 2005, 2010 and 2013 floods, the Mediterranean was a substantial moisture source in the August 2002 flood, especially in the early stages, as shown by James et al. (2004) and Gangoiti et al. (2011b). The sensitivity study of Messmer et al. (2017) points towards the particular role of the Mediterranean Sea in contrast to other moisture sources like the North Atlantic. Thus, the role of the Mediterranean seems to be variable across events. Overall, these Vb-events reveal quite diverse moisture source regions which might be related, however, to the choice of analysed events.

In the existing scientific literature only the above mentioned floods triggered by Vb-cyclones in recent years (2002, 2005, 2010, and 2013) have been analysed quantitatively in terms of the evaporative moisture source regions. In this study, we extended these case studies by investigating the moisture uptake during in total 16 Vb-events from 1901 to 2010 with focus on flood-producing precipitation in the Danube, Elbe, and Odra catchment regions. The moisture source diagnostics was based on a computationally demanding Lagrangian approach. Thus, it could not be applied to all Vb-cyclones from 1901 to 2010 that we detected in our dataset ( $> 10^3$  events). For all Vb-cyclones, instead, we analysed the characteristics like evaporation, SST or soil moisture content in the moisture uptake regions identified with our 16 case studies. In doing so, we could investigate how source region characteristics differ for Vb-cyclones with high or low precipitation in the selected catchment regions. More specifically, in this study, we address the following research questions:

1. What are the evaporative moisture source regions of flood-causing precipitation in synoptic situations with Vb-cyclones?
2. Which characteristics in the moisture source regions intensify the precipitation in synoptic situations with Vb-cyclones?

As a data basis, we use the ERA-20C reanalysis data (Poli et al. 2016) that was dynamically downscaled over Europe

with a high resolution and interactively coupled regional atmosphere-ocean model (COSMO-CLM+NEMO, Akhtar et al. 2019; Kelemen et al. 2019; Primo et al. 2019). We tracked the cyclone pathways according to Wernli and Schwierz (2006) and Sprenger et al. (2017) to identify Vb-events. The evaporative moisture source regions were quantified based on a Lagrangian analysis with Lagranto (Sprenger and Wernli 2015; Wernli and Davies 1997) and a moisture source diagnostic (Sodemann et al. 2008) for 16 selected Vb-events from 1901 to 2010 (Sect. 3.2). The characteristics of identified moisture source regions were investigated for all detected Vb-events during 1901–2010 ranked with respect to their precipitation impact in the Danube, Elbe, and Odra river catchments (Sect. 4). We discuss our findings and open research questions in section 5. Finally, we revisit the key findings of this paper in Sect. 6.

## 2 Data and methods

### 2.1 Dynamically downscaled ERA-20C reanalysis

The analysis was based on the ECMWF twentieth century reanalysis (ERA-20C; Poli et al. 2016) that assimilates surface pressure and marine surface wind measurements. The horizontal resolution is about 125 km (spectral triangular truncation T159; Poli et al. 2016). Vb-cyclones are strongly influenced by mountains (e.g., Aebischer and Schär 1998; Trigo et al. 2002) and heavy rainfall is especially triggered along the east-west oriented mountain ranges (Grams 2014). A higher spatial and temporal resolution is necessary to capture such local-scale processes involved in orographically induced precipitation. Therefore, the ERA-20C reanalysis was dynamically downscaled to a horizontal resolution of about 12 km ( $\Delta x = 0.11^\circ$ ; Krug et al. 2020). The highest mountain in the Alps (Ore Mountains) is the Mont Blanc (the Klínovec) with about 4800 m (1244 m) altitude. In our downscaled reanalysis, the highest gridpoint in the Alps (Ore Mountains) was more realistically represented with 2960 m (792 m) compared to 1434 m (392 m) in ERA-20C reanalysis (provided at  $0.75^\circ$  horizontal grid-spacing; please note that the original resolution is a spectral truncation T159). The downscaled reanalysis covers an extended EURO-CORDEX domain (Giorgi et al. 2009) and continuously spans the years from 1901 to 2010. The temporal resolution of the output variables ranges from hourly for variables such as total precipitation and surface temperature to daily for variables such as daily maximum 2 m temperature.

The dynamical downscaling was performed with the regional climate model COSMO-CLM (Consortium for Small-scale Modelling in Climate Mode; Rockel et al. 2008) which was interactively coupled with the regional ocean model NEMO (Nucleus for European Modeling of

the Ocean; Madec and the NEMO Team 2016) over the marginal seas (Mediterranean Sea, North Sea, and Baltic Sea) to better represent the components of the water cycle. The freshwater inflow of rivers routing into the Mediterranean Sea (except for the Nile) was implemented with the river routing model TRIP (Total Runoff Integrating Pathways; Oki and Sud 1998) to close the regional water budget (so that, e.g., the Mediterranean salinity is consistent with precipitation over land; Sevault et al. 2014). The lateral boundary conditions were given by the ERA-20C reanalysis data with a one-way Davies (1976) relaxation scheme. We applied no spectral nudging within the regional climate model (RCM) domain to avoid discontinuities in the internal RCM variability and to account for the computational constraints of a coupled RCM covering 110 years. More details about the model setup and performance can be found in Primo et al. (2019).

### 2.2 Vb-cyclone tracking and event selection

We applied the method by Wernli and Schwierz (2006) and refined in Sprenger et al. (2017) to track all cyclones at mean sea level pressure with a 3-hourly resolution in the dynamically downscaled ERA-20C reanalysis (interpolated to  $0.5^\circ$  with bilinear interpolation of Climate Data Operators, CDO, Schulzweida 2021) from 1901 to 2010 within  $25^\circ \text{W}$ – $45^\circ \text{E}$  and  $25^\circ$ – $75^\circ \text{N}$ . Cyclones were identified based on closed sea-level pressure isobars. The position of the deepest pressure within a closed isobar defined the cyclone centre. The cyclone centres at different time steps were connected to cyclone tracks. More specifically, the position of the following track point was detected by a first guess approach based on the previous displacement vector. The cyclone centre nearest to the first guess within a search radius smaller than 1000 km was then assigned as a new track point. Cyclone track points where topography exceeds 1500 m were excluded because of the extrapolation errors of the mean surface pressure values from these altitudes (Wernli and Schwierz 2006). We excluded spurious cyclones with a life time shorter than 24 h. For simplicity, all cyclones crossing northward the  $47^\circ \text{N}$  latitude between  $12^\circ \text{E}$  and  $22^\circ \text{E}$  were classified as Vb-cyclones (cf. Hofstätter and Blöschl 2019) as shown in Fig. S1. We detected in total 1107 Vb-cyclones between 1901 and 2010 in our dynamically downscaled reanalysis, which corresponds to about ten Vb-cyclones per year. The average Vb-cyclone lifetime was about 44 h. The average core pressure was about 1003 hPa and the deepest core pressure was about 958 hPa.

We extended the previous case studies of widespread floods associated with Vb-cyclones (mentioned in the introduction) based on the detected Vb-cyclone events since 1901. For the first time, we analysed the moisture source regions of 16 selected Vb-cyclone events during the early

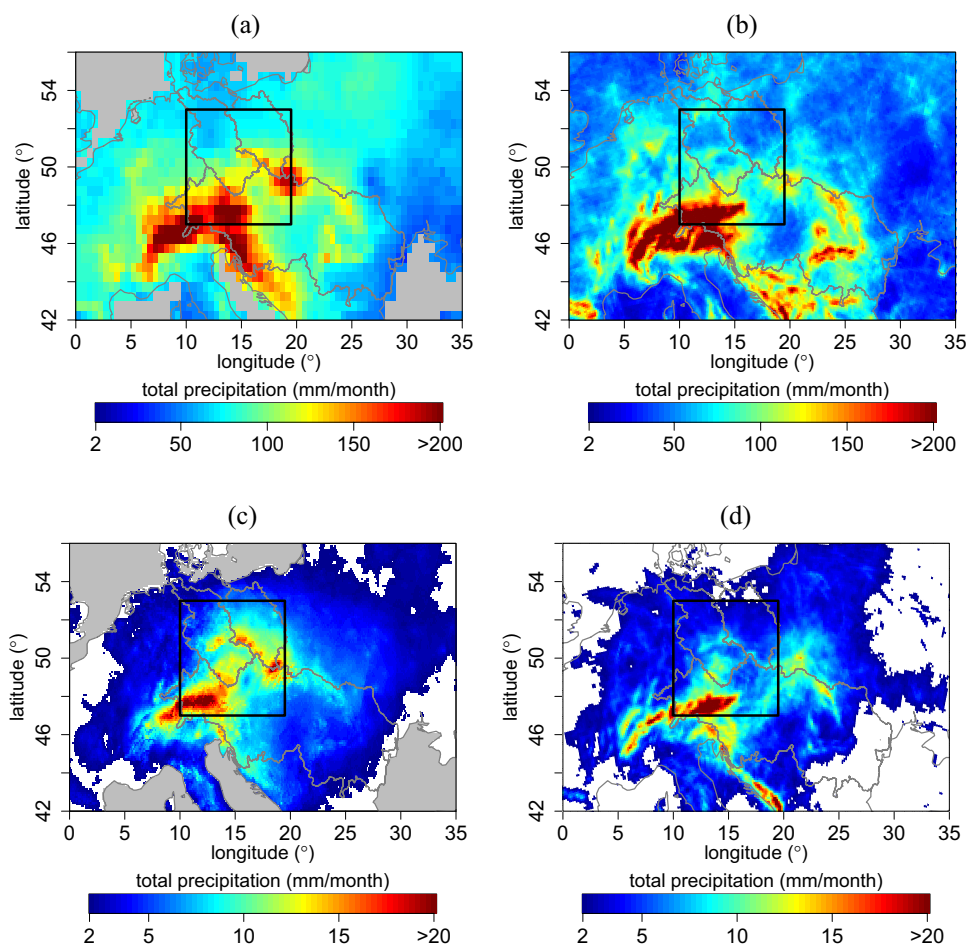
decades of the past century (Table 1, e.g., in 1903 and 1954; Stahl and Hofstätter 2018). By selecting events throughout the past century, we could investigate whether the detected contributions of the European continent and North Atlantic Ocean in previous studies depend on the few selected events in literature. We compared the detected Vb-cyclone tracks (Fig. S2) and simulated precipitation sums with historical flood events to select the events of interest in this study. As a reference, we used the Climatic Research Unit Timeseries (CRU TS v4.04, Harris et al. 2020) and E-OBS v 22.0e (Cornes et al. 2018) gridded observation data. We calculated monthly sums for the events prior to 1950 to fit the temporal resolution of CRU observation data (monthly precipitation sums due to data availability in the early decades of the past century).

For defining the days for our moisture source diagnostics, we analysed the total precipitation sums in the domain of 10° E, 19.5° E, 47° N, and 53° N (including the catchment regions of interest, black rectangle in Fig. 1) and selected the 4 consecutive days of most intense rainfall. Please note that 4 days do not directly correspond to the detected cyclone track period, since only parts of the cyclone pathway were detected with our cyclone tracking (Fig. S2). All selected

events occurred from May to August except for the flood in October 1930 (see Table 1, and references therein). We detected Vb-cyclone events with heavy precipitation predominantly during the summer half-year. Exceptions with high precipitation amounts during the winter half-year were the Vb-events during 25.12.1993 and 26.12.1993 (Danube, 54th highest precipitation anomaly) or during 21.11.1962 and 22.11.1962 (Odra, 5th highest precipitation anomaly) associated with heavy snow fall in Central Europe (e.g., snow height increase from 0 cm on 21.11.1962 to 21 cm on 24.11.1962 in Berlin-Buch; Climate Data Center, version v005, 2017, DWD). These winter events were not included in this study focusing on the summer-half year.

The events in August 2002 and July 1954 were the most prominent ones in the past century besides the Central European flood in June 2013 (Blöschl et al. 2013). The latter one was excluded from our analysis because the ERA-20C reanalysis only covers the years from 1900 to 2010. Other events, such as the flood in June 1936 or June 1979, were less intense but still affecting more than one river catchment. Some events mentioned in Stahl and Hofstätter (2018) were not included because the associated Vb-cyclone trajectories and precipitation sums were

**Fig. 1** Monthly precipitation sums in **a** CRU-observational data and **b** the dynamically downscaled ERA-20C data averaged over July 1903, June 1926, October 1930, June 1936, and May 1949. The lower panels show the precipitation sums during the selected events No. 6–16 (from start to end date) in **c** E-OBS observational data and **d** the dynamically downscaled ERA-20C data. Missing values are shown with grey colour



not captured well enough in the dynamically downscaled reanalyses (e.g., the May 1940 flood and the July 1985 event). We also excluded events that were limited to a relatively small region (e.g., flood in northeastern Switzerland in June 1910 and the Vistula region in July 2001). The influence of the local catchment conditions is less pronounced for floods affecting more than one macro-scale river catchment, and the meteorological circumstances (such as heavy precipitation) dominate. In addition to the flood events mentioned in Stahl and Hofstätter (2018), past flood events associated with synchronous peak discharges in the Danube and Elbe catchment were selected, such as the event in July 1965 and July 1981 (see Fig. 2).

### 2.3 Lagrangian moisture source diagnostics of selected cases

This study used a Lagrangian approach to identify the evaporative moisture source regions of 16 selected precipitation events associated with floods. We analysed 4 days of heavy precipitation for each event (Table 1). Figure 3 shows the corresponding mean total precipitation with a slight eastward shift throughout the events. During these 4 days, we calculated for every hour 7-day three-dimensional backward trajectories with Lagranto (Wernli and Davies 1997; Sprenger and Wernli 2015) based on model

**Fig. 2** Temporal evolution of simulated mean daily precipitation sums in the region of 10° E, 19.5° E, 47° N, and 53° N (including all selected river catchments regions of interest, black rectangles in Fig. 1) and daily GRDC river discharges measured at Dresden (Elbe) and Hofkirchen (Danube) **a** during the August 1977 event, **b** the July 1977 event, **c** the August 2002 event, and **d** averaged over all events listed in Table 1. We defined the start dates and end dates of our analyses (marked with dashed lines; see also Table 1) so that they cover the 4 days of the highest rainfall amounts in advance of the peak discharges

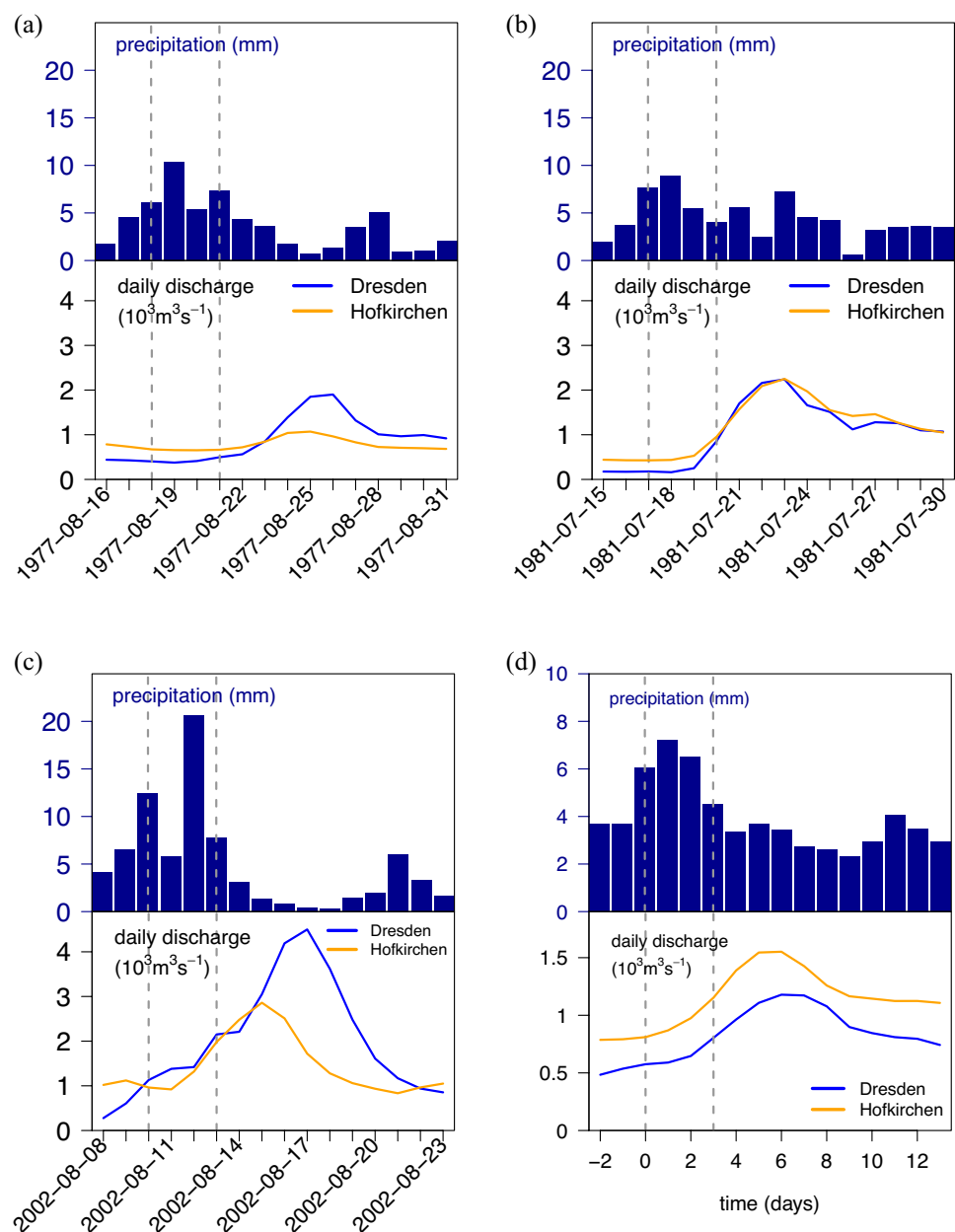


**Table 1** Floods in Central Europe associated with Vb-cyclones and the start and end date of the 4-day heavy precipitation period analysed with the Lagrangian moisture diagnostics

No.	Start date	End date	Selected references
1	11.07.1903	14.07.1903	Keller (1903), Fischer (1904), Hellmann and von Elsner (1911)
2	23.06.1926	26.06.1926	Sorg (1926), Fabian and Bartels (1928), Fickert (1932)
3	26.10.1930	29.10.1930	Friedrich (1930), Weichmann (1931), Fickert (1932)
4	02.06.1936	05.06.1936	Fischer (1938, p. 330), Drews et al. (2003, Abb. 2-1)
5	20.05.1949	23.05.1949	Kresser (1957, Tab. 1)
6	30.06.1954	03.07.1954	Blöschl et al. (2013), Böer et al. (1959)
7	21.07.1957	24.07.1957	Becker and Grünwald (2003)
8	09.06.1965	12.06.1965	Uhlemann et al. (2010), Gvoždíková and Müller (2017)
9	18.08.1977	21.08.1977	Naumann et al. (1978), Böhm and Wetzel (2006)
10	16.06.1979	19.06.1979	Uhlemann et al. (2010)
11	17.07.1981	20.07.1981	Uhlemann et al. (2010), Akhtar et al. (2019)
12	31.05.1986	03.06.1986	Ionita et al. (2015)
13	17.07.1997	20.07.1997	Kundzewicz et al. (1999), Hofstätter and Chimani (2012)
14	10.08.2002	13.08.2002	Sodemann et al. (2009), Gangoiti et al. (2011a, b, 2015), Ulbrich et al. (2003a)
15	20.08.2005	23.08.2005	Winschall (2013, Chapter 3), Akhtar et al. (2019)
16	15.05.2010	18.05.2010	Winschall et al. (2014)

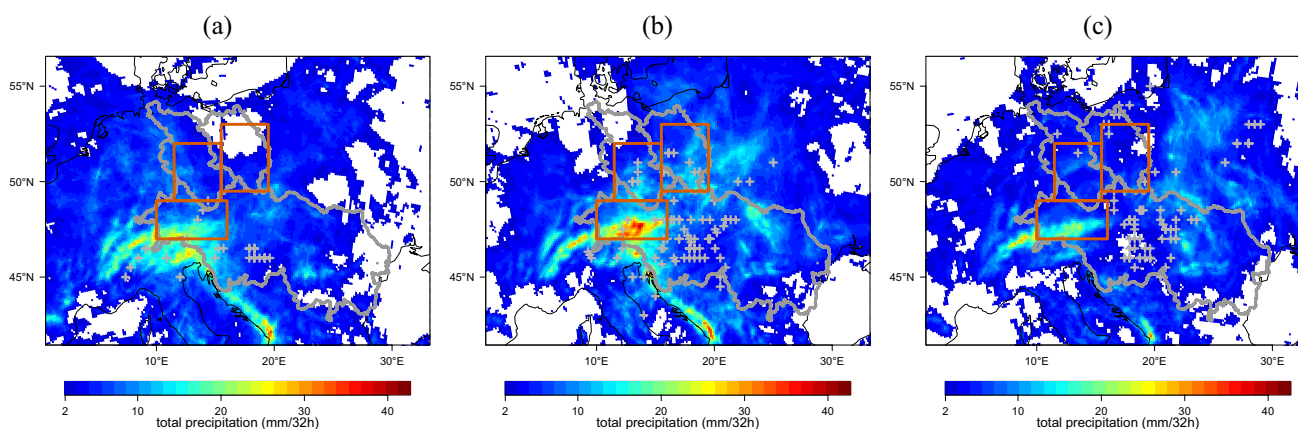


**Fig. 3** Mean total precipitation sum of the selected 4-day (96 h) Vb-events (Table 1) in the dynamically downscaled reanalysis split into three event phases of 32 h each (from a to c). The grey crosses mark

the corresponding Vb-cyclone centre positions. The orange rectangles show the backtracking start point regions within the selected regions in the Danube, Elbe, and Odra catchments (grey polygons)

level data with the height based hybrid vertical coordinate. We chose 7 days because this is above the global mean atmospheric moisture residence time of about 4–5 days (Läderach and Sodemann 2016). For periods shorter than 5 days, the moisture source region diagnostic would not give robust results. We did not use more than 7-days backward trajectories because then the majority of backward trajectories left the domain of our downscaled reanalysis. Potentially relevant moisture sources from outside the regional domain were therefore neglected. In summer and autumn this share is most likely negligible, whereas in winter more long-range transport and influence from the North Atlantic outside the domain can be expected (Aemisegger et al. 2014). In total about  $16 \times 10^3$  to  $18 \times 10^3$  starting points were

selected equidistantly every 15 km in the horizontal on 39 vertical levels from 250 to 9750 m a.s.l. in the Danube, Elbe, and Odra catchment regions, respectively (Fig. 3, orange rectangles). This high temporal and spatial resolution is crucial to capture relevant air streams, for example, around the Alps. We traced specific humidity and other meteorological variables like wind, temperature, or the planetary boundary layer height along the trajectories for air parcels exceeding 80% relative humidity at their arrival point in the selected catchment regions. In this way, only trajectories related to high relative humidity and thus precipitation were considered (cf. Grams et al. 2014).

The evaporative moisture source regions were then identified by changes of specific humidity along the air parcel

trajectories, assuming that changes of specific humidity result from evaporation and precipitation (Sodemann et al. 2008). The individual moisture uptakes were weighted according to the method of Sodemann et al. (2008), i.e., the contribution of each moisture uptake is reduced by following moisture uptakes and precipitation events along the air parcel trajectory. With such an approach based on 3D trajectories, the amount of dynamical lifting (such as orographic and frontal lifting) is considered. These processes are relevant in Vb-cyclone precipitation (Ulbrich et al. 2003b). In accordance with Aemisegger et al. (2014) and Winschall et al. (2014), we analysed the moisture uptake of air parcels irrespective of altitude, not only within the boundary layer but also above. Some uptakes above the boundary layer may actually be linked to surface evaporation via convection, which in fact might be of high relevance during summer. The explained fraction of moisture uptake was on average about 75% and limited by the domain of the dynamically downscaling. Finally, the total event moisture uptake was obtained by weighting the hourly moisture source contributions of each trajectory with its associated precipitation.

The moisture diagnostics were applied to the hourly trajectories during the respective 4 days listed in Table 1, that means in total 96 moisture uptake maps were calculated per flood event and river catchment. In terms of land sources, we differentiated between the selected Danube, Elbe, and Odra river catchment regions (orange rectangles in Fig. 3) and the rest of the continent to analyse the temporal evolution of various moisture source contributions. Furthermore, we distinguished between the Mediterranean Sea (7° E, 22° E, 35° N, 46° N, grey polygon in Fig. 4, sea grid points only), the North Sea and the Baltic Sea (50° N, 58.5° N, 30° E, 0° E, grey polygon in Fig. 4, sea grid points), the North Atlantic (20° W, 0° W, 40° N, 60° N, grey polygon in Fig. 4, sea grid points), the Black Sea, and other oceanic source regions. We did not select the whole Mediterranean Basin as region of interest but only the domain where the main moisture uptake in our case studies occurred. This corresponds to the findings of Krug et al. (2021) in which the selected Mediterranean region was found to play a key role for precipitation formation in the Odra (Poland) catchment area.

## 2.4 Climatological Analysis

Besides the above mentioned 16 case studies, we analysed for all 1107 Vb-cyclones during 1901–2010 the evaporation, SSTs, soil moisture content at 4–10 cm, and wind speeds in the predefined moisture source regions. We calculated daily anomalies with respect to the analysis period (1901–2010) to remove the seasonal cycle and to account for possible systematic biases in the dynamically downscaled ERA-20C reanalysis. The spatial and temporal averages were calculated for each Vb-cyclone life time and pre-defined uptake region.

For improved readability of the figures, we calculated the moving averages over 50 events and the local LOESS regression (Local Polynomial Regression Fitting; Cleveland et al. 1992) with corresponding prediction intervals based on the R software package *stats* v4.0.2 (R Core Team 2013). Moreover, we ranked all Vb-cyclones according to their total precipitation within the Danube, the Elbe, and Odra river catchment regions to gain more insights in processes associated with Vb-cyclones causing heavy precipitation compared to Vb-events with only low or normal precipitation.

## 3 Case studies

### 3.1 Selected events from 1901 to 2010

Figure 1 shows the total precipitation sums of the selected events of interest (Table 1) in comparison to gridded CRU (Harris et al. 2020) and E-OBS (Cornes et al. 2018) observation data. The total precipitation events were captured by our dynamically downscaled ERA-20C reanalysis, even though the total precipitation sums over the Odra and Elbe catchment region were underestimated. As expected, Vb-cyclones often induce floods affecting more than one macro-scale river catchment. Figure 2 shows the synchronous occurrence of observed peak discharges in the Elbe and Danube river catchment and the preceding rainfall in our dynamically downscaled ERA-20C reanalysis for selected events and the average discharges and simulated precipitations sums for all selected events in our study (Table 1).

Among the selected events, highest peak discharges occurred in the Elbe and Danube river catchments on the 17.08.2002 with  $4.50 \times 10^3 \text{ m}^3 \text{ s}^{-1}$  at the gauge Dresden (15.08.2002,  $2.86 \times 10^3 \text{ m}^3 \text{ s}^{-1}$ , Hofkirchen; Fig. 2c), on the 12.07.1954 with  $2.30 \times 10^3 \text{ m}^3 \text{ s}^{-1}$  (13.07.1954,  $3.29 \times 10^3 \text{ m}^3 \text{ s}^{-1}$ , Hofkirchen), and on the 23.07.1981 with  $2.24 \times 10^3 \text{ m}^3 \text{ s}^{-1}$  (23.07.1981,  $2.25 \times 10^3 \text{ m}^3 \text{ s}^{-1}$ , Hofkirchen; Fig. 2b). Highest daily precipitation anomalies were simulated in our dynamically downscaled reanalysis for the August 2005 event (rank 17 in the selected Elbe region, rank 49 in the Danube region), the October 1930 event (rank 21 in the Elbe region), the July 1981 event (rank 35 in the Danube region), and the May 1986 event (rank 46 in the Odra catchment). During May 2010 precipitation anomalies of rank 80/93/99 were simulated in the Odra/Danube/Elbe catchment region of interest. In our simulation, also other Vb-events were associated with large precipitation anomalies but no widespread Vb-flood was reported, for example, between 08.08.2007 and 10.08.2007 (rank 100, Danube catchment). That event was associated with flooding in Switzerland, but no Vb-cyclone was mentioned in literature (Bezzola and Ruf 2009), even though we detected one Vb-cyclone with our less restrictive definition compared to Hofstätter et al. (2016). A cutoff low

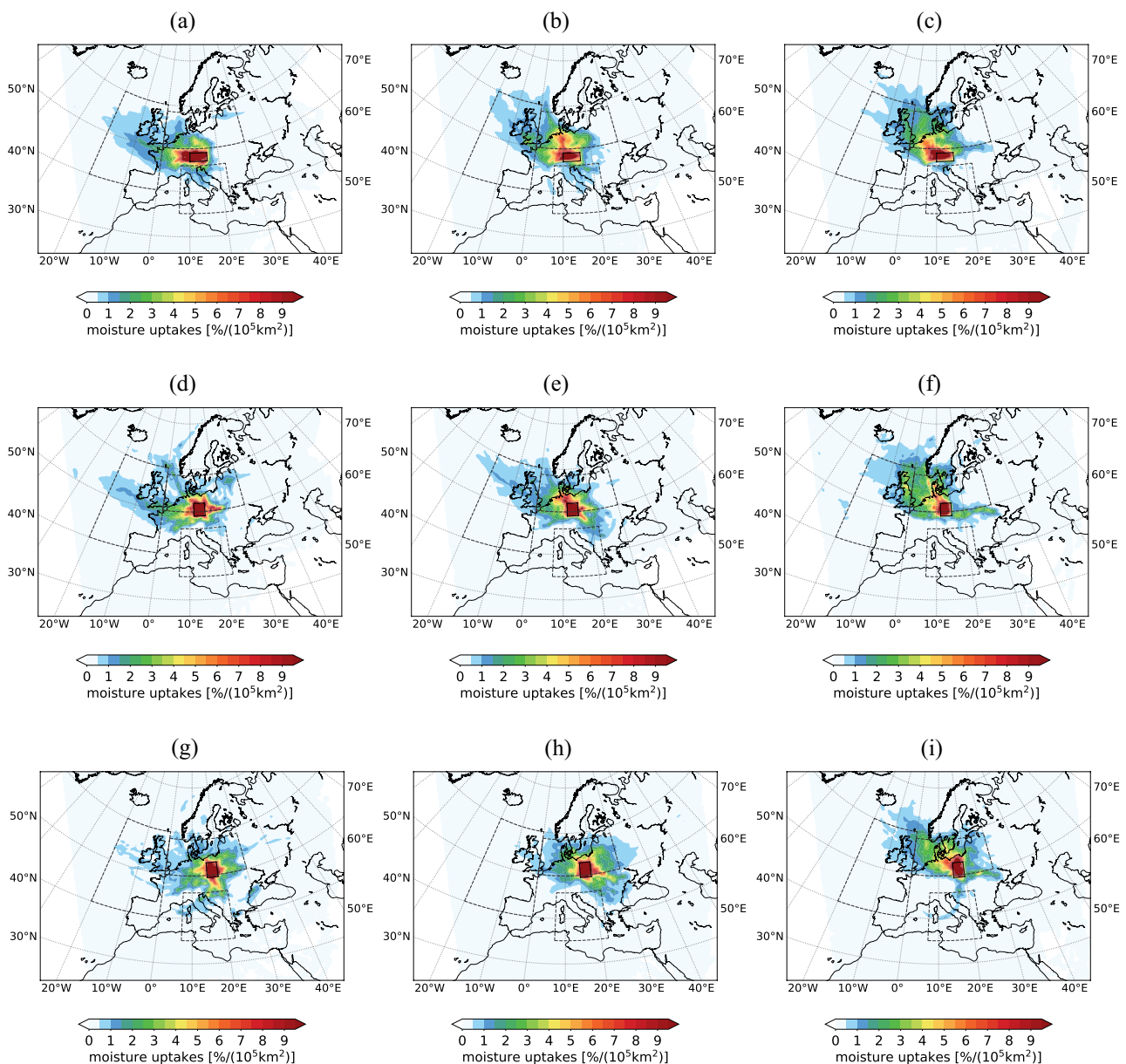


**Fig. 4** Moisture uptakes for precipitation in the Danube (panels a–c), Elbe (d–f), and Odra catchment (g–i) averaged over the events listed in Table 1. The columns show the time means of the first event phases (a, d, g), the middle (b, e, h), and the last event phases (c, f, i) with

32 h each. The integral over the entire moisture source region sums up to 100% of the explained moisture. The boxes show the domains of the moisture source regions in Fig. 5

was located over the Alpine region in August 2007 (Bezzola and Ruf 2009)—a synoptic situation that is often associated with Vb cyclones causing heavy precipitation (e.g., Messmer et al. 2015; Hofstätter et al. 2018; Mittermeier et al. 2019). Potential causes for a discrepancy between observed flood events and simulated precipitation impact are a shift in the precipitation field, over- or underestimated precipitation sums (Fig. 1), enhanced or decreased pre-saturation of the affected river catchments in the reanalysis data. Nonetheless,

the dynamically downscaled reanalysis represents a physically consistent atmospheric data set.

### 3.2 Evaporative moisture source regions of 16 selected cases

Figure 4 shows the average relative moisture uptake for the events listed in Table 1 with a focus on precipitation in (a–c) the Danube, (d–f) the Elbe, and (g–i) the Odra catchment. Throughout the three event phases, the moisture uptake



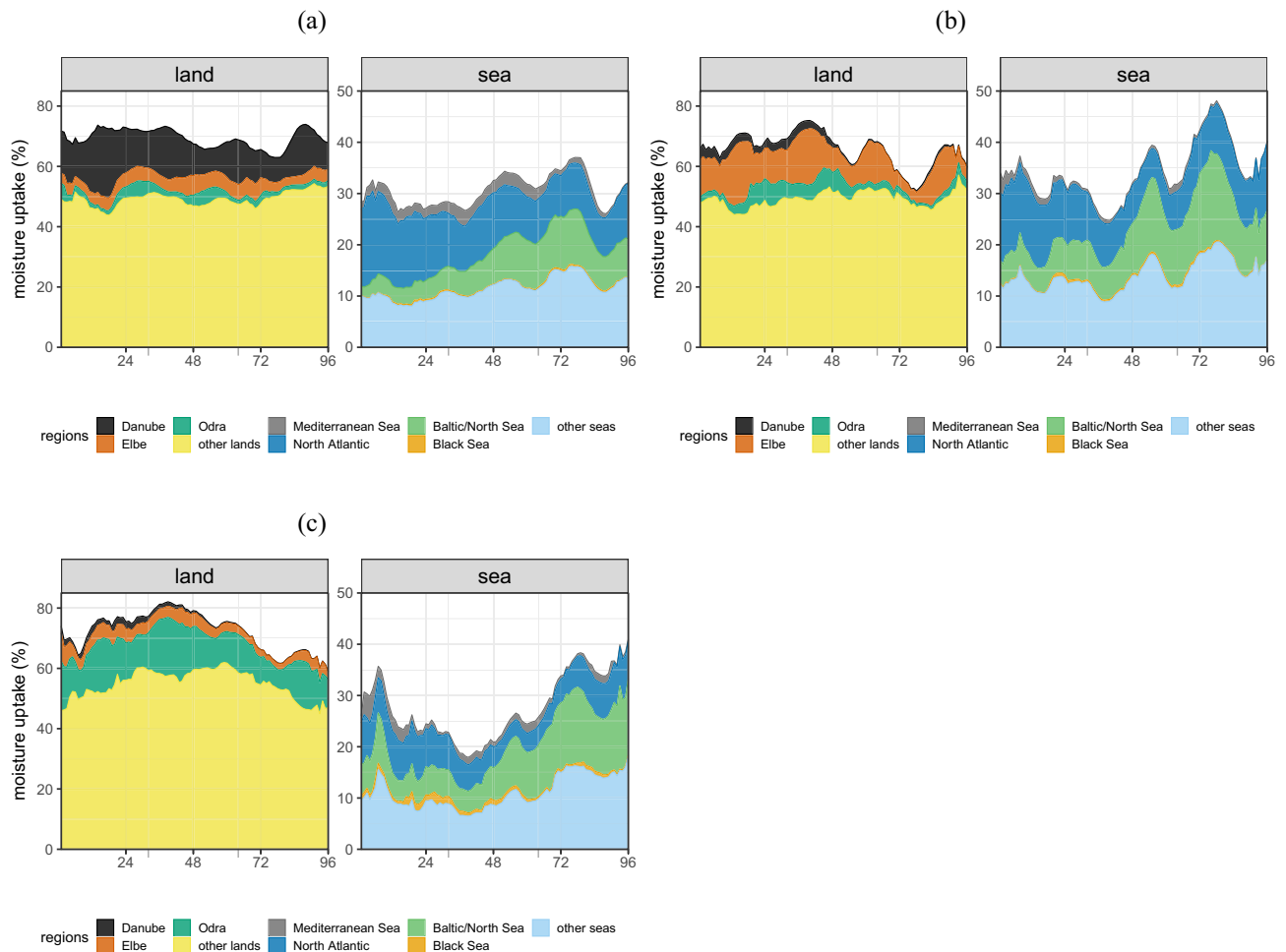


**Fig. 5** Relative percentage contribution of various moisture source regions to precipitation in the **a** Danube, **b** Elbe, and **c** Odra catchment averaged over all 16 events listed in Table 1. The x-axis cor-

responds to the 4 days of heavy precipitation selected for the moisture diagnostics. Note the different y-axis scales for land and sea source regions

was largest within the selected catchment region and surrounding continental surface. Overall, the moisture uptake over the European continent contributed to about 50–80% of the precipitation falling in the selected river catchment area (Fig. 5) and up to 90% during individual events (e.g., Fig. 6c). Later in the Vb-event, the cyclone centres recurve towards the Elbe and Odra catchment, leading to more precipitation north of the Alps (Fig. 3b, c). At this stage, more moisture can be transported from the Baltic Sea and the North Sea south-eastwards to the river catchments (Fig. 4). The contribution of the North Sea and Baltic Sea increased throughout the events, whereas the proportion of the North Atlantic and the land moisture uptake decreased accordingly (Figs. 4 and 5, Elbe catchment).

The percental moisture uptake within the respective river catchment was only up to 20%, even though the intensity of these local uptakes were comparatively large considering the limited areal extent of the catchment (Supplement, Fig. S3).

Interestingly, the eastern North Atlantic and the North Sea/Baltic Sea showed the highest moisture contribution among the marginal seas with up to 17% and 20% moisture uptake, respectively (Figs. 4, 5). These moisture source regions correspond to summer mean moisture sources of the Alpine region (Sodemann and Zubler 2010, using 20-day backward trajectories). The North Atlantic Ocean contribution might be associated with another extratropical cyclone or the large-scale moisture transport, because we quantified the moisture uptake of all precipitation within the river catchment areas, not only the one related to the Vb-cyclone. For the July 1997 event, Akhtar et al. (2019) pointed to the fact that the flood-producing rainfall was not only linked to a Vb-cyclone but also another cyclone over the North Sea. The North Atlantic/North Sea contribution could also be linked to the northerly flow on the western side of the trough that is often involved in triggering cyclogenesis of the Vb-cyclones south of the Alps. The exact transport pathway of this northerly moisture,

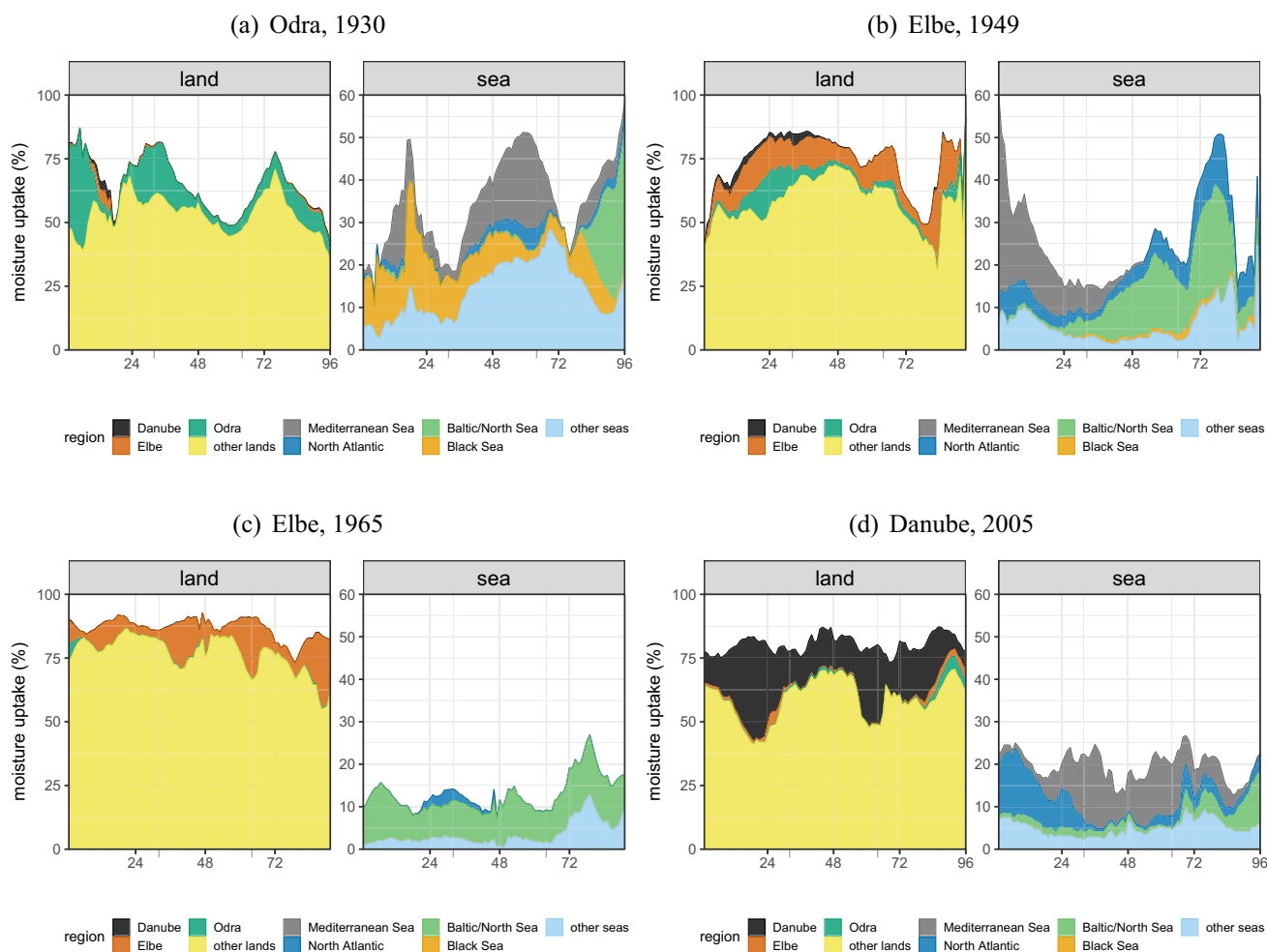


**Fig. 6** As in Fig. 5, but for selected events and catchment regions

however, is still unclear. It might be moisture contributing to stratiform precipitation behind the cold front, or it could be moisture that was advected into the warm sector of the Vb-cyclone.

The Black Sea contributed to precipitation during the 1930 (Fig. 6a), 1949, and 2005 events, especially in the Odra catchment (Supplement, Figs. S4–S6). The mean moisture uptake over the Black Sea in general was highest for the Odra catchment but accounted only for up to 2% of the moisture uptake (Fig. 5c).

As mentioned in the introduction, because of the Vb-cyclone pathway a large contribution from the Mediterranean Sea might be expected. Here we find that the Mediterranean Sea, however, played overall only a minor role and affected more the Danube and Odra catchment than the Elbe region (Figs. 4 and 5). Nonetheless, the Mediterranean Sea was a significant oceanic source during the 1930 flood, the 1949 flood (Fig. 6b), and the 2005 flood for the selected river catchment regions, and during the 2002 event, the Mediterranean Sea contributed significantly to the Odra catchment.

In contrast, we detected no moisture uptake over the Mediterranean Sea for precipitation in the Danube, Elbe, and Odra catchment during 1965 (Fig. 6c), 1986, or the 2010 event. The temporal evolution of the moisture uptake in different regions reveals that, on average, the moisture uptake from the Mediterranean Sea contributed to the flood-triggering heavy precipitation during the event start and decreased towards the end (Fig. 5). That corresponds—together with an increasing influence of the North Sea and Baltic Sea during the events—to the Vb-cyclone pathway from the Mediterranean Sea to Central Europe. For some events, however, the event evolution was completely different. For example, the Mediterranean Sea was an important moisture source for precipitation in the Danube catchment only towards the end of the 1977 event. Another example is the August 2005 flood, during which the Mediterranean contribution was large in the middle of the event in the Danube catchment (Fig. 6d). In the Elbe and Odra catchments, the Mediterranean Sea was a relevant moisture source during the last 2 days of that event (Supplement, Figs. S5, S6).

In summary, the European continent is found to be by far the largest moisture source for the chosen 16 case studies of heavy precipitation events in the selected catchments. The major oceanic source regions were the North Atlantic and North Sea/Baltic Sea. Our results for Vb-cyclone events correspond to the climatological source regions. Sodemann and Zubler (2010) analysed the moisture sources of precipitation in the European Alpine region during 1995–2002 with 20-day backward trajectories and detected the North Atlantic Ocean, the Mediterranean Sea, the North Sea, the Baltic Sea, and the European land surface, with the European land surfaces dominating during the summer season. These findings are in accordance with the study by Aemisegger et al. (2014).

The Mediterranean Sea played only a minor role as a source region, averaged over all selected Vb-cyclone events, but it is a region with a large variability in its contribution. More Vb-events have to be analysed to gain further insights into the role of the specific processes in the moisture source regions of precipitation in synoptic situations with Vb-cyclones in the selected river catchment regions. Therefore, a climatological perspective is adopted in the next section to investigate the moisture source conditions of Vb-cyclones that triggered heavy precipitation compared to Vb-events that were associated with low or normal precipitation.

#### 4 Climatology of Vb-events from 1901 to 2010

In this section, we discuss the distinct characteristics of heavy precipitation producing Vb-events compared to normal Vb-events. Therefore, we ranked all Vb-cyclones according to their precipitation in the Danube, Elbe, and Odra river catchment regions (Fig. 7). The ranked precipitation anomalies show a steep increase for the highest ranked events in all river catchment regions (Fig. 7, the daily climatology of 1901–2010 was removed for calculating the anomalies presented in this section). The Elbe, and Odra catchment have similar rainfall characteristics due to their close spatial location to each other. In contrast, the selected Danube catchment region is in the vicinity of the Alps favouring orographic lifting and is usually affected earlier by the Vb-cyclone than the Elbe and Odra region due to the typical cyclone pathway around the eastern side of the Alps (Fig. S2). Therefore, some moisture already rains out along the Alpine fringe before air masses propagate north-eastwards (Figs. 1, 3), which reduces the direct moisture contribution of the Mediterranean Sea. Thus, the Danube catchment shows a higher variability with lower minimum values

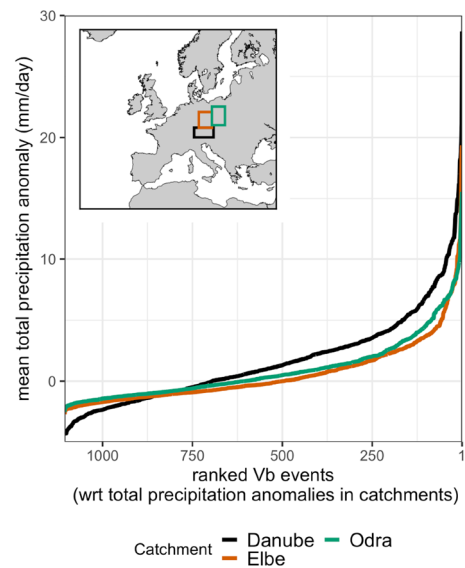


**Fig. 7** Ranked total precipitation anomalies in the Danube, Elbe, and Odra catchment during each Vb-cyclone from 1901 to 2010

and overall higher precipitation anomalies for medium and high-ranked events in Fig. 7.

In the following sections, we adopt this ranking of the Vb-cyclones for analysing the continental and oceanic moisture source conditions. We focus firstly on the moisture source conditions within the river catchments, such as soil moisture and the diurnal evaporation range, because the area-weighted uptakes were comparatively high (Sect. 4.1). Secondly, we discuss the properties of the oceanic moisture sources like ocean evaporation, the SST, and wind speed (Sect. 4.2).

##### 4.1 River catchments

High daily amplitudes of evapotranspiration together with positive soil-moisture anomalies can point towards an increased efficiency of convective precipitation processes (Schär et al. 1999). Figure 8a shows the anomaly of the diurnal evaporation range  $E_{\max} - E_{\min}$  during all Vb-events from 1901 to 2010 ranked according to the precipitation amount. Indeed, the anomalies of the diurnal evaporation range were larger for high precipitation Vb-cyclones, especially in the Danube catchment. That indicates that processes within the river catchment regions, such as the soil moisture-precipitation feedback and convective rainfall, might play a role, even though the moisture uptake was only up to 20% of the precipitation in the river catchments of interest in our case study. Similarly, these processes are probably relevant in other continental moisture source regions.

Figure 8b shows the daily soil moisture anomalies at 4–10 cm soil depth averaged over the respective Vb-events.

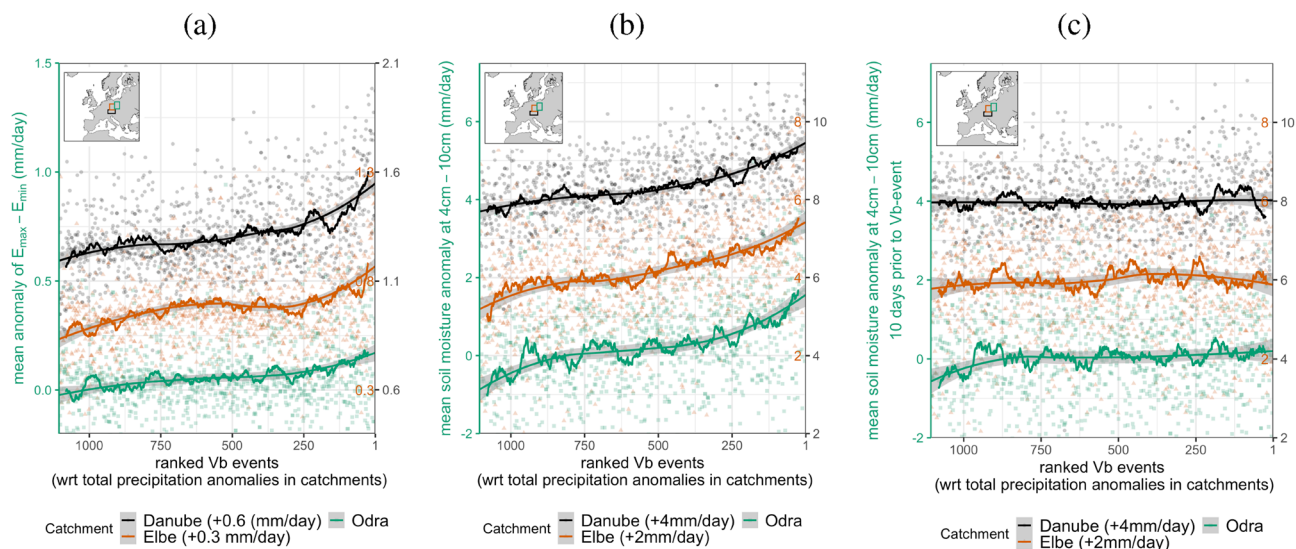


**Fig. 8** a Anomalies of diurnal evaporation range  $E_{\max} - E_{\min}$  and b soil moisture anomalies during the corresponding ranked Vb-events. c Soil moisture anomalies 10 days prior to the respective Vb-events.

The lines show the moving average and the LOESS regression. Note, the data for Danube and Elbe catchment were shifted by constant values for improved readability

This soil depth reacts relatively fast to rainfall events. Results were similar for other soil layers except for deeper layers with more than 1 m depth (not shown). All river catchments show an increase of soil moisture anomalies from low to high precipitation Vb-cyclones. Rainfall during the respective Vb-events increases the soil moisture content, which is an important ingredient for local moisture uptake in the river catchment and over the rest of the continent.

On the contrary, the soil moisture conditions 10 days preceding the event shows no positive anomaly for heavy precipitation events (Fig. 8c). Only in the Odra catchment, low precipitation Vb-events correspond with drier antecedent soil conditions. Thus, mainly the event precipitation itself triggered the moisture uptake within the river catchments. Nonetheless, case studies like the one in Ho-Hagemann et al. (2015), analysing the July 1997 event, indicate some exceptions with precipitation linked to preceding soil moisture conditions.

## 4.2 Marginal seas

In our 16 case studies (Sect. 3), the eastern North Atlantic and the North Sea/Baltic Sea were the largest oceanic moisture source regions with a moisture uptake of up to 17% and 20% of the precipitation falling in the selected river catchments. Figure 9, middle and right panel, show the conditions of these moisture source regions during all ranked 1107 Vb-cyclones from 1901 to 2010 in terms of anomalies in oceanic evaporation, SST, and wind speed. Interestingly, the evaporation anomalies in the North Atlantic and the North Sea/Baltic Sea vary around zero and show no difference

for Vb-cyclones with low precipitation compared to Vb-cyclones with heavy precipitation. That is also the case for SST and wind speed anomalies. For all river catchments, the wind speed anomalies over the North Sea/Baltic Sea and the North Atlantic are negative or close to zero and induce therefore no evaporation enhancement.

Even though the Mediterranean Sea explained on average only up to 5% of the precipitation in the selected river catchments in our case studies (Sect. 3.2), remarkable anomalies in evaporation, and wind speed show distinct differences between heavy precipitation and low-to-normal precipitation Vb-cyclones. The evaporation anomalies over the Mediterranean Sea were higher for Vb-cyclones with heavy precipitation in all river catchments (Fig. 9, left panel). The overall increase is highest for the Danube catchment, likely because of the closest vicinity of this catchment to the Mediterranean Sea. Interestingly, these positive evaporation anomalies were associated with positive wind speed anomalies. The Spearman rank correlation coefficient  $R$  (Spearman 1904) for evaporation and wind speed anomalies over the selected Mediterranean region was about +0.7 ( $p < 0.01$ ) for the 300 highest ranked precipitation events in all selected catchment regions (Fig. 10). Positive wind speed anomalies and dynamic evaporative forcing are usually associated with negative SST anomalies (Fig. 10). The Mediterranean SSTs and wind speed anomalies are weakly negatively correlated ( $R$  ranging from  $-0.25$  to  $-0.3$  for the 300 highest precipitation events, Fig. 10). We discuss this in more detail in the following section and the result that, even though the Mediterranean Sea was only a minor moisture source region, an enhanced and dynamically driven moisture uptake was

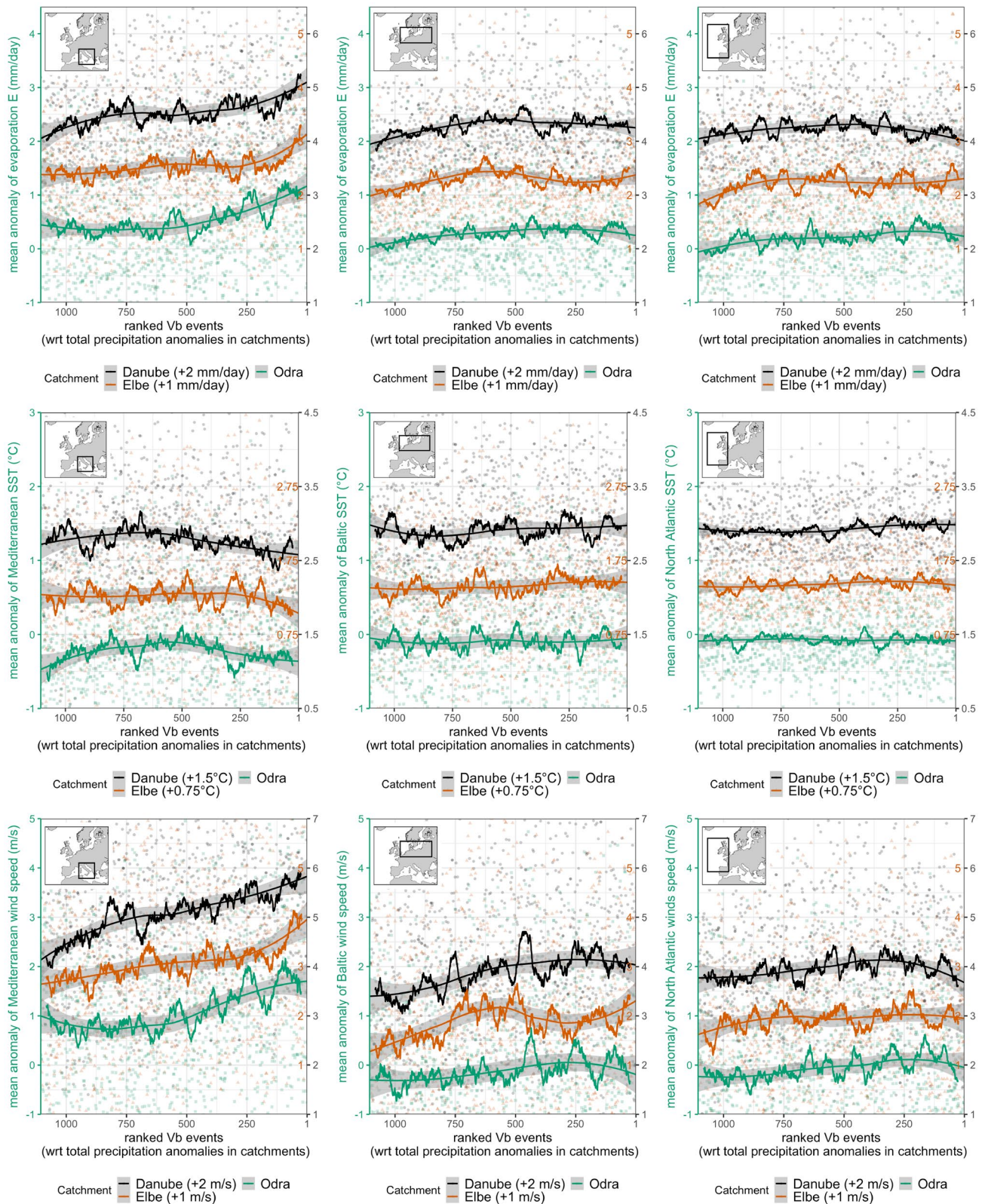


**Fig. 9** Anomalies of evaporation (upper row), sea surface temperatures (middle), and wind speed (lower row) in (left) the Mediterranean Sea, (middle) the North Sea and Baltic Sea, and (right) the North Atlantic during the corresponding ranked Vb-events. The lines

show the moving average and the LOESS regression. Note, the data for Danube and Elbe catchment were shifted by a constant value for improved readability

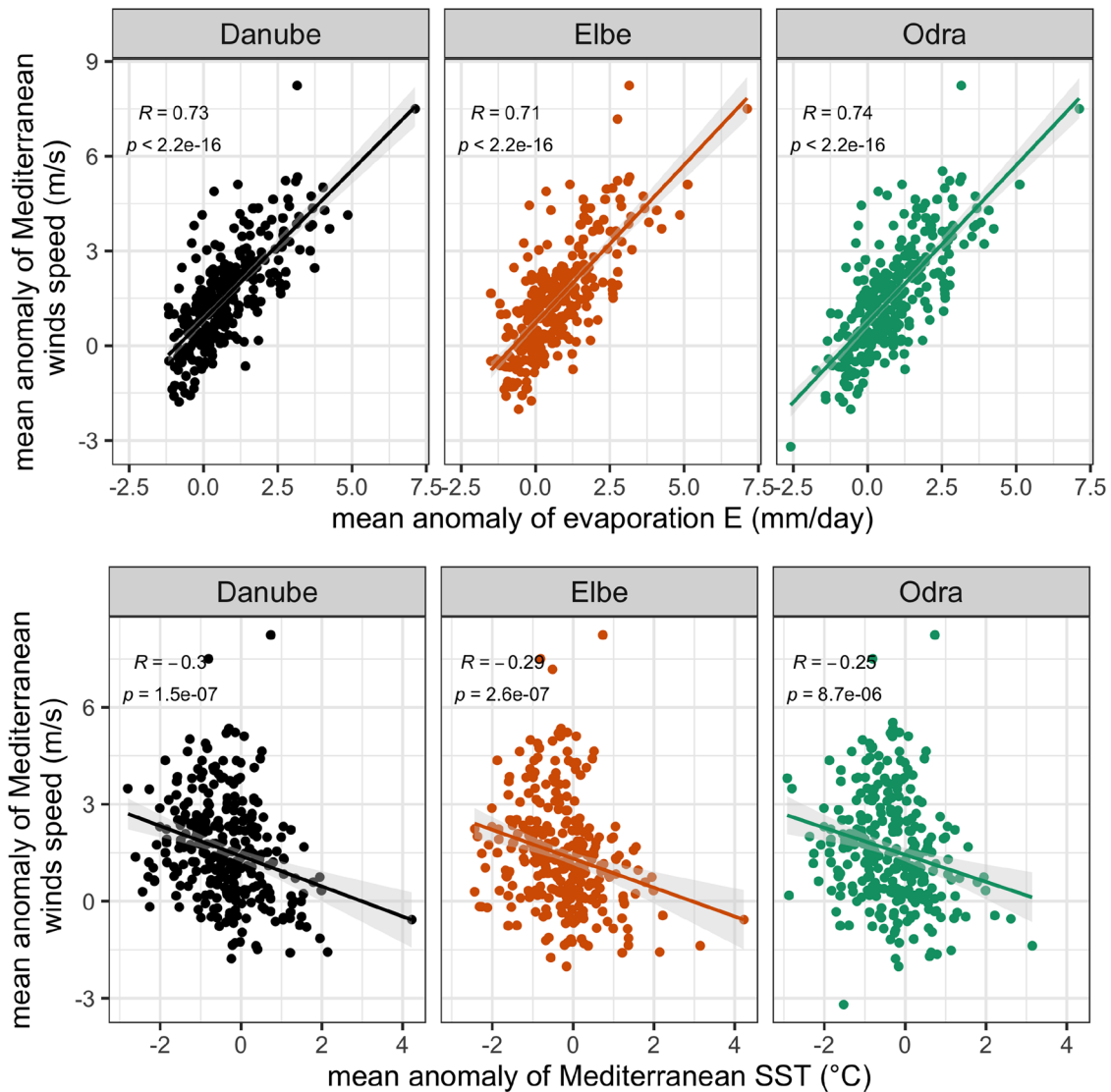


**Fig. 10** Scatter plots of Mediterranean evaporation, wind speed, and SST anomalies for the 300 highest ranked precipitation events with the Spearman's rank correlation coefficient  $R$  (Spearman 1904)

observed for heavy precipitation in synoptic situations with Vb-cyclones.

## 5 Discussion

Due to the Vb-cyclone pathway from the Mediterranean Sea north-eastwards to Central Europe, one might expect a high moisture contribution of the Mediterranean Sea to precipitation in Central Europe. Indeed, the studies of James et al. (2004) and Gangoiti et al. (2011b) detect a substantial contribution of the Mediterranean Sea for the initial phase of the August 2002 flood. However, case studies on other floods such as the ones in May 2010 or May/June 2013 reveal only minor moisture uptakes over the Mediterranean Sea (Grams

et al. 2014; Winschall et al. 2014; Kelemen et al. 2016). Our moisture source diagnostics of 16 Vb-cyclone events during 1901–2010 (Table 1) further supports this finding (Fig. 5).

Based on the minor moisture uptake one might deduce that the Mediterranean Sea plays only a minor role for precipitation in synoptic situations with Vb-cyclones in Central Europe. However, the study of Messmer et al. (2017) shows increased precipitation with higher Mediterranean SSTs while an increase of North Atlantic SST has only marginal impact. Our climatological analysis reveals that heavy precipitation in weather situations with Vb-cyclones in the selected Danube, Elbe, and Odra catchment regions were associated with positive evaporation anomalies over the Mediterranean Sea, whereas the North Atlantic and the North Sea/Baltic Sea evaporation anomalies showed

no correlation with the Vb-event ranks. Thus, in synoptic situations with Vb-cyclones, anomalously high evaporation over the Mediterranean Sea is linked with high precipitation in Central Europe, even though the moisture uptake contribution was relatively small during the selected cases of Vb-cyclone events in Sect. 3. This is in accordance with Ciric et al. (2018) concluding that the Mediterranean Sea contribution to precipitation in Central Europe is similar for extreme events compared to the climatological mean. The short-range transport of this moisture evaporated over the Mediterranean Sea could contribute to Vb-cyclone intensification in the early stages of their development through latent heat release. The confluence of the moist Mediterranean air masses with other, relatively cold and dry air masses could intensify the frontal zones of the Vb-cyclone, especially during the presence of an upper-level trough over Central Europe (e.g., Grams et al. 2014). The Mediterranean moisture might also play a key role in pre-moistening continental moisture source regions that later on contribute to heavy precipitation downstream in the Danube, Elbe, and Odra catchments.

Interestingly, we detected a dynamically driven evaporation enhancement in synoptic situations with Vb-cyclones with heavy precipitation in our selected catchment regions. A similar behaviour was observed during strong evaporation events in the subpolar North Atlantic (Aemisegger 2018). On the other hand, higher SSTs can be associated with higher evaporation, which might be the reason for the weakly negative correlation between SST and wind speed anomalies. High absolute SSTs during the initial phase of the Vb-cyclone may contribute to an increase of the precipitation in weather situations with Vb-cyclones in the early stages of the cyclone development via enhanced upward moisture fluxes and a decreased atmospheric stability (cf. Messmer et al. 2017).

The SST effect emphasizes the possible impact of the Mediterranean Sea on precipitation in synoptic situations with Vb-cyclones in Central Europe, in particular in the context of rising SSTs in a warming climate (Giorgi 2006). Moreover, these processes partly explain the seasonal distribution of extreme Vb-flood events occurring predominantly during summer, when absolute SSTs over the Mediterranean Sea are usually high (cf. Messmer et al. 2017). Besides, we detected only a few Vb-events with high precipitation anomalies during the winter.

In our case studies, the diagnosed moisture sources depend strongly on the selected region of precipitation. For example, the moisture uptake over the Mediterranean Sea contributed in August 2005 to about 20% of the precipitation in the Danube catchment, but only to about 5% in the Elbe catchment (Figs. 6d, S5). Thus, the findings of our study may not be representative for other catchments and regions in Europe. Another shortcoming of our study is that

we could not detect multiple precipitation and re-evaporation cycles with our Lagrangian moisture diagnostics. To gain more insights, one could perform backtracking and moisture source diagnostics for the preceding precipitation events, that built up the soil moisture contributing to the moisture uptake during the event of interest. However, this requires iterative moisture source diagnostics covering several months in advance of the event. In this study, some of the continental moisture uptakes might originate, for instance, from Mediterranean moist air masses that precipitated out upstream of our catchment regions earlier. Besides, we focused exclusively on the precipitation impact and detected no differences in the preceding soil moisture conditions for Vb-events with high or small precipitation. For flood producing events, however, the antecedent soil conditions and initial hydraulic load are important ingredients, as it was the case during June 2013 (Schröter et al. 2015).

## 6 Conclusions

Even though Vb-cyclones have a frequency of about two to ten events per year, only a few cause extreme flooding. These floods are among the most devastating ones in the Danube, Elbe, and Odra river catchments (e.g., the Elbe flood in August 2002). Our study aimed at shedding light on intensification processes of the precipitation inducing such extreme floods. Therefore, we quantified the moisture source regions of 16 historical floods linked to Vb-cyclones with a Lagrangian approach. Additionally, we analysed the moisture source characteristics during all 1107 Vb-cyclones in our dynamically downscaled ERA-20C data from 1901 to 2010. In the following, we answer the research questions of our study:

1. **What are the evaporative moisture source regions of flood-causing precipitation in synoptic situations with Vb-cyclones?** For all 16 case studies, a mixture of different moisture source regions was observed. Overall, up to 80% of the precipitation originated from the continental surface, with the highest continental uptake within the respective river catchments (when taking the spatial extent into account) triggered mainly by the event precipitation itself (indicating important local precipitation recycling). Other main uptake regions were the North Sea/Baltic Sea and North Atlantic with up to 20% contribution. On average, the moisture contribution of the North Sea and the Baltic Sea increased, while the contribution of the North Atlantic and the continental surface decreased accordingly during the Vb-event evolution (likely linked to the cyclone centre recurving towards northern and eastern Central Europe).

The Black Sea was a minor source region, affecting the Odra river catchment, in a few cases. Also the Mediterranean Sea was only a minor source region on average. That supports previous case studies on selected flood events triggered by Vb-cyclones (e.g., Sodemann et al. 2009; Winschall et al. 2014; Grams et al. 2014; Kelemen et al. 2016). The relative importance of moisture source regions was highly variable for the individual events and river catchments. In particular, the share of Mediterranean moisture was highly variable from event to event. This highlights the complex dynamical interplay of different air masses leading to convergence of moisture during particularly severe Vb-floods.

2. **Which characteristics in the moisture source regions intensify the precipitation in synoptic situations with Vb-cyclones?** Remarkably, the anomalies in evaporation, SSTs, and wind speed over the North Atlantic and North Sea/Baltic Sea showed no distinct trend with precipitation in synoptic situations with Vb-cyclones in the Odra, Elbe, and Danube river catchment regions. Conversely, Vb-cyclones with high precipitation amounts were associated with positive evaporation anomalies over the Mediterranean Sea, even though the diagnosed moisture uptake in that region was relatively small in our case studies. Interestingly, these evaporation anomalies were dynamically driven and therefore linked with positive wind speed anomalies.

Overall, an enhanced and dynamically driven moisture uptake over the Mediterranean Sea was found to be characteristic for Vb-events with heavy precipitation, even though the dominating moisture uptake regions were the European continent and the North Atlantic and the North Sea/Baltic Sea. Possible underlying processes are beyond the focus of this study. In future studies, it would be interesting to analyse how short-range moisture transport from the Mediterranean Sea and resulting latent heat release could intensify Vb-cyclones during the early stages of the cyclone development. It could be beneficial to distinguish between the moisture source regions of precipitation linked solely to Vb-cyclones (extreme and common ones), as opposed to other systems to gain deeper insights into the role of the Mediterranean Sea. For this, a suitable approach could be the consideration of a radius around the analysed cyclones (e.g., Messmer et al. 2020). Besides, further research is needed on the role of latent heat release later in the Vb-cyclone life cycle for prolonging atmospheric blockings (e.g., Pfahl et al. 2015; Steinfeld and Pfahl 2019; Steinfeld et al. 2020) that may trigger the development of new Vb-cyclones (Hofstätter and Blöschl 2019). It will be also an issue of future research to quantify the role of convective precipitation for summer time intensification of precipitation during Vb-cyclones (e.g., Grams

et al. 2014; Messmer et al. 2015), also in the context of soil-precipitation feedback (Schär et al. 1999; Ho-Hagemann et al. 2015) which enhances the efficiency of convective precipitation within the river catchment.

The dynamically driven moisture uptake over the Mediterranean Sea highlights the importance of high-resolution regional climate simulations for improved wind fields in the Mediterranean Sea (Herrmann et al. 2011; Obermann et al. 2018). Coupled regional atmosphere-ocean models can further improve the representation of air-sea interactions and thus cyclone characteristics, as demonstrated for selected Medicane events in Akhtar et al. (2014).

**Supplementary Information** The online version contains supplementary material available at <https://doi.org/10.1007/s00382-022-06256-7>

**Acknowledgements** The authors thank Cristina Primo, Goethe University Frankfurt (now at Deutscher Wetterdienst, Germany), for providing us dynamically downscaled ERA-20C reanalysis data. The financial support of the German Research Foundation (Deutsche Forschungsgemeinschaft, DFG) in terms of the research group FOR 2416 Space-Time Dynamics of Extreme Floods (SPATE) is gratefully acknowledged. The authors acknowledge the Deutsches Klimarechenzentrum (DKRZ) and the Center for Scientific Computing (CSC) for supplying us with computational facilities. Furthermore, we thank the European Environment Agency (EEA) for sharing the European river catchments (ERC) shapefiles and the International Commission for Protection of Danube River (ICPDR) for the information on the Danube catchment. We acknowledge the E-OBS dataset from the EU-FP6 project UERRA (<http://www.uerra.eu>) and the Copernicus Climate Change Service, and the data providers in the ECA&D project (<https://www.ecad.eu>). We thank the Climatic Research Unit (CRU) for providing the CRU TS gridded observation data.

**Author Contributions** The software for the moisture source diagnostics was written by FA. The data collection and analysis was performed by AK. All authors discussed the results and contributed to the study conception. The first draft of the manuscript was written by AK and all authors commented on previous versions of the manuscript. All authors read and approved the final manuscript. Funding acquisition by BA.

**Funding** Open Access funding enabled and organized by Projekt DEAL. Amelie Krug and Bodo Ahrens acknowledge support by the German Research Foundation (Deutsche Forschungsgemeinschaft, DFG) in terms of the research group FOR 2416 Space-Time Dynamics of Extreme Floods (SPATE). This work used resources of the Deutsches Klimarechenzentrum (DKRZ) granted by its Scientific Steering Committee (WLA) under project ID bb1064.

**Availability of data and material (data transparency)** The Vb-cyclone tracks used for this study are available for research purposes in the zenodo archive (<https://doi.org/10.5281/zenodo.4333258>). Moisture uptakes of our case studies are available upon request from Amelie Krug.

## Declarations

**Conflicts of interest/Competing interests** The authors declare that they have no conflict of interest.



**Code availability (software application or custom code)** The source code of Lagranto (Wernli and Davies 1997; Sprenger and Wernli 2015) is available under [www.lagranto.ethz.ch](http://www.lagranto.ethz.ch). The cyclone tracking method of Wernli and Schwierz (2006) and refined in Sprenger et al. (2017) is available on request from Michael Sprenger. The source code of the moisture source diagnostics is available upon request from Franziska Aemisegger.

**Open Access** This article is licensed under a Creative Commons Attribution 4.0 International License, which permits use, sharing, adaptation, distribution and reproduction in any medium or format, as long as you give appropriate credit to the original author(s) and the source, provide a link to the Creative Commons licence, and indicate if changes were made. The images or other third party material in this article are included in the article's Creative Commons licence, unless indicated otherwise in a credit line to the material. If material is not included in the article's Creative Commons licence and your intended use is not permitted by statutory regulation or exceeds the permitted use, you will need to obtain permission directly from the copyright holder. To view a copy of this licence, visit <http://creativecommons.org/licenses/by/4.0/>.

## References

- Aebischer U, Schär C (1998) Low-level potential vorticity and cyclogenesis to the lee of the Alps. *J Atmos Sci* 55(2):186–207 [https://doi.org/10.1175/1520-0469\(1998\)055<0186:LLPVAC>2.0.CO;2](https://doi.org/10.1175/1520-0469(1998)055<0186:LLPVAC>2.0.CO;2)
- Aemisegger F (2018) On the link between the North Atlantic storm track and precipitation deuterium excess in Reykjavik. *Atmos Sci Lett* 19(12):e865. <https://doi.org/10.1002/asl.865>
- Aemisegger F, Pfahl S, Sodemann H, Lehner I, Seneviratne SI, Wernli H (2014) Deuterium excess as a proxy for continental moisture recycling and plant transpiration. *Atmos Chem Phys* 14(8):4029–4054. <https://doi.org/10.5194/acp-14-4029-2014>
- Akhtar N, Brauch J, Dobler A, Béranger K, Ahrens B (2014) Medicanes in an ocean-atmosphere coupled regional climate model. *Nat Hazard* 14(8):2189–2201. <https://doi.org/10.5194/nhess-14-2189-2014>
- Akhtar N, Krug A, Brauch J, Arsouze T, Dieterich C, Ahrens B (2019) European Marginal Seas in a regional atmosphere-ocean coupled model and their impact on Vb-cyclones and associated precipitation. *Clim Dyn*. <https://doi.org/10.1007/s00382-019-04906-x>
- Becker A, Grünwald U (2003) Disaster management: flood risk in Central Europe. *Science* 300(5622):1099. <https://doi.org/10.1126/science.1083624>
- Bezzola GR, Ruf W (eds) (2009) Ereignisanalyse Hochwasser August 2007. Analyse der Meteo- und Abflussvorhersagen; vertiefte Analyse der Hochwasserregulierung der Jurarandgewässer. Umwelt-Wissen Nr. 0927, Bundesamt für Umwelt, Bern, 209 S
- Blöschl G, Nester T, Komma J, Parajka J, Perdigão R (2013) The June 2013 flood in the Upper Danube Basin, and comparisons with the 2002, 1954 and 1899 floods. *Hydrol Earth Syst Sci* 17(12):5197–5212. <https://doi.org/10.5194/hess-17-5197-2013>
- Böer W, Schubert H, Wilser O (1959) Das Sommerhochwasser der Elbe im Juli 1954. Mitteilungen zum Deutschen Gewässerkundlichen Jahrbuch Nr 19 Akademie-Verlag, Berlin
- Böhm O, Wetzel KF (2006) Flood history of the Danube tributaries Lech and Isar in the Alpine foreland of Germany. *Hydrol Sci J* 51(5):784–798. <https://doi.org/10.1623/hysj.51.5.784>
- Ciric D, Nieto R, Losada L, Drumond A, Gimeno L (2018) The Mediterranean Moisture contribution to climatological and extreme monthly continental precipitation. *Water* 10(4):519. <https://doi.org/10.3390/w10040519>, <http://www.mdpi.com/2073-4441/10/4/519>
- Cleveland WS, Grosse E, Shyu WM (1992) Statistical models in S, Wadsworth & Brooks/Cole, chap Local regression models, p 68. <https://doi.org/10.1201/9780203738535>
- Cornes RC, van der Schrier G, van den Besselaar EJM, Jones PD (2018) An ensemble version of the E-OBS temperature and precipitation data sets. *J Geophys Res Atmos* 123(17):9391–9409. <https://doi.org/10.1029/2017JD028200>
- Davies HC (1976) A lateral boundary formulation for multi-level prediction models. *Q J R Meteorol Soc* 102(432):405–418. <https://doi.org/10.1002/qj.49710243210>
- Drews I, Hangen-Brodersen C, zum Kley-Fiquet B (2003) Hochwassersvorsorge in Deutschland – Lernen aus der Katastrophe 2002 im Elbegebiet, Schriftenreihe des DKKV, vol 29. Deutsches Komitee für Katastrophenvorsorge e. V. (DKKV), Bonn
- Fabian W, Bartels G (1928) Das Hochwasser der Oder im Sommer 1926, vol 5. Berlin
- Fickert R (1932) Die Hochwässer in der Sächsischen Lausitz im Juni 1926 und Oktober/November 1930. *Wasserkraft und Wasserwirtschaft* 27(21/22/23):241–245, 258–262, 272–274, münchen and Berlin
- Fischer K (1904) Entstehung und Verlauf des Oderhochwassers im Juli 1903. *Geograph Z* 10:316–332 (leipzig)
- Fischer G (1938) Centralblatt für Bakteriologie, Parasitenkunde und Infektionskrankheiten. 141–142
- Friedrich W (1930) Die Wasserstandsverhältnisse der norddeutschen Stromgebiete im Oktober und im Gesamtabflußjahr 1930. *Zentralblatt der Bauverwaltung* 50(50):873, berlin
- Gangoiti G, Gómez-Domenech I, Sáez De Cámara E, Alonso L, Navazo M, Iza J, García JA, Ilardia JL, Millán MM (2011a) Origin of the water vapor responsible for the European extreme rainfalls of August 2002: 2. A new methodology to evaluate evaporative moisture sources, applied to the August 11–13 central European rainfall episode. *J Geophys Res Atmos* 116(D21):1–16. <https://doi.org/10.1029/2010JD015538>
- Gangoiti G, Sáez de Cámara E, Alonso L, Navazo M, Gómez MC, Iza J, García JA, Ilardia JL, Millán MM (2011b) Origin of the water vapor responsible for the European extreme rainfalls of August 2002: 1. High-resolution simulations and tracking of air masses. *J Geophys Res Atmos*. <https://doi.org/10.1029/2010JD015530>
- Gangoiti G, Sáez de Cámara E, Gómez-Domenech I, Alonso L, Navazo M, Iza J, García JA, Millán MM (2015) Re-evaluation of moisture sources for the August 2002 extreme rainfall episode in central Europe: evaporation from falling precipitation included in a mesoscale modeling system. *J Hydrol* 529(P3):696–710. <https://doi.org/10.1016/j.jhydrol.2015.08.055>
- Giorgi F (2006) Climate change hot-spots. *Geophys Res Lett* 33(8):L08707. <https://doi.org/10.1029/2006GL025734>
- Giorgi F, Jones C, Asrar G (2009) Addressing climate information needs at the regional level: the CORDEX framework. *WMO Bull* 58(3):175–183
- Grams CM, Binder H, Pfahl S, Piaget N, Wernli H (2014) Atmospheric processes triggering the central European floods in June 2013. *Nat Hazard* 14(7):1691–1702. <https://doi.org/10.5194/nhess-14-1691-2014>
- Gvozdíková B, Müller M (2017) Evaluation of extensive floods in western/central Europe. *Hydrol Earth Syst Sci* 21(7):3715–3725. <https://doi.org/10.5194/hess-21-3715-2017>
- Harris I, Osborn TJ, Jones P, Lister D (2020) Version 4 of the CRU TS monthly high-resolution gridded multivariate climate dataset. *Sci Data* 7(1):109. <https://doi.org/10.1038/s41597-020-0453-3>, <http://www.nature.com/articles/s41597-020-0453-3>

- Hellmann G, von Elsner G (1911) Meteorologische Untersuchungen über die Sommerhochwasser der Oder, vol 230. Veröffentlichungen des Königlich Preußischen Meteorologischen Instituts. [https://doi.org/10.1007/978-3-662-25325-0\\_xI\\_236](https://doi.org/10.1007/978-3-662-25325-0_xI_236)
- Herrmann M, Somot S, Calmanti S, Dubois C, Sevault F (2011) Representation of spatial and temporal variability of daily wind speed and of intense wind events over the Mediterranean Sea using dynamical downscaling: impact of the regional climate model configuration. *Nat Hazard* 11(7):1983–2001. <https://doi.org/10.5194/nhess-11-1983-2011>
- Hofstätter M, Blöschl G (2019) Vb cyclones synchronized with the Arctic-/North Atlantic Oscillation. *J Geophys Res Atmos* 124(6):3259–3278. <https://doi.org/10.1029/2018JD029420>
- Hofstätter M, Chimani B (2012) Van Bebber's cyclone tracks at 700 hPa in the Eastern Alps for 1961–2002 and their comparison to Circulation Type Classifications. *Meteorol Z* 21(5):459–473. <https://doi.org/10.1127/0941-2948/2012/0473>
- Hofstätter M, Chimani B, Lexer A, Blöschl G (2016) A new classification scheme of European cyclone tracks with relevance to precipitation. *Water Resour Res* 52(9):7086–7104. <https://doi.org/10.1002/2016WR019146>
- Hofstätter M, Lexer A, Homann M, Blöschl G (2018) Large-scale heavy precipitation over central Europe and the role of atmospheric cyclone track types. *Int J Climatol* 38(S1):e497–e517. <https://doi.org/10.1002/joc.5386>
- Ho-Hagemann HTM, Hagemann S, Rockel B (2015) On the role of soil moisture in the generation of heavy rainfall during the Oder flood event in July 1997. *Tellus Ser A Dyn Meteorol Oceanogr*. <https://doi.org/10.3402/tellusa.v67.28661>
- Ionita M, Dima M, Lohmann G, Scholz P, Rimbu N (2015) Predicting the June 2013 European flooding based on precipitation, soil moisture, and sea level pressure. *J Hydrometeorol* 16(2):598–614. <https://doi.org/10.1175/JHM-D-14-0156.1>
- James P, Stohl A, Spichtinger N, Eckhardt S, Forster C (2004) Climatological aspects of the extreme European rainfall of August 2002 and a trajectory method for estimating the associated evaporative source regions. *Nat Hazards Earth Syst Sci* 4(5/6):733–746. <https://doi.org/10.5194/nhess-4-733-2004>
- Kelemen FD, Ludwig R, Meyers M, Ulbrich S, Pinto JG (2016) Evaluation of moisture sources for the Central European summer flood of May/June 2013 based on regional climate model simulations. *Tellus Ser A Dyn Meteorol Oceanogr*. <https://doi.org/10.3402/tellusa.v68.29288>
- Kelemen FD, Primo C, Feldmann H, Ahrens B (2019) Added value of atmosphere-ocean coupling in a century-long regional climate simulation. *Atmosphere* 10(9):537. <https://doi.org/10.3390/atmos10090537>
- Keller H (1903) Die Hochflut in der Oder vom Juli 1903, ihre Ursachen und die Abwehr der Hochwasser-Gefahren. *Dtsch Bauztg* 37(90/91):580–584 (, **586–592, berlin**)
- Kresser W (1957) Die Hochwässer der Donau, Schriftenreihe des Österreichischen Wasserwirtschaftsverbandes, vol 32/33. Springer Verlag, Wien
- Krug A, Primo C, Fischer S, Schumann A, Ahrens B (2020) On the temporal variability of widespread rain-on-snow floods. *Meteorol Z* 29(2):147–163. <https://doi.org/10.1127/metz/2020/0989>
- Krug A, Pothapakula PK, Primo C, Ahrens B (2021) Heavy Vb-cyclone precipitation: a transfer entropy application showcase. *Meteorol Z* 30(3):279–284. <https://doi.org/10.1127/metz/2021/1071>
- Kundzewicz ZW, Szamalek K, Kowalczyk P (1999) The Great Flood of 1997 in Poland. *Hydrol Sci J* 44(6):855–870. <https://doi.org/10.1080/02626669909492285>
- Läderach A, Sodemann H (2016) A revised picture of the atmospheric moisture residence time. *Geophys Res Lett* 43(2):924–933. <https://doi.org/10.1002/2015GL067449>
- Madec G, the NEMO Team (2016) NEMO Ocean Engine. Note du Pôle de modélisation de l'Institut Pierre-Simon Laplace No 27, Paris. ISSN No 1288-1619
- Messmer M, Gómez-Navarro JJ, Raible CC (2015) Climatology of Vb cyclones, physical mechanisms and their impact on extreme precipitation over Central Europe. *Earth Syst Dyn* 6(2):541–553. <https://doi.org/10.5194/esd-6-541-2015>
- Messmer M, Gómez-Navarro JJ, Raible CC (2017) Sensitivity experiments on the response of Vb cyclones to sea surface temperature and soil moisture changes. *Earth Syst Dyn* 8(3):477–493. <https://doi.org/10.5194/esd-8-477-2017>
- Messmer M, Raible CC, Gómez-Navarro JJ (2020) Impact of climate change on the climatology of Vb cyclones. *Tellus A Dyn Meteorol Oceanogr* 72(1):1–18. <https://doi.org/10.1080/16000870.2020.1724021>
- Mittermeier M, Braun M, Hofstätter M, Wang Y, Ludwig R (2019) Detecting climate change effects on Vb cyclones in a 50-member single-model ensemble using machine learning. *Geophys Res Lett* 46(24):14653–14661. <https://doi.org/10.1029/2019GL084969>
- Naumann A, Sujata H, Krause K, Seeger U (1978) Sommerhochwasser der Oder 1977. *Wasserwirtschaft - Wassertechnik* 28:21–57
- Nissen KM, Ulbrich U, Leckebusch GC (2013) Vb cyclones and associated rainfall extremes over Central Europe under present day and climate change conditions. *Meteorol Z* 22(6):649–660. <https://doi.org/10.1127/0941-2948/2013/0514>
- Obermann A, Bastin S, Belamari S, Conte D, Gaertner MA, Li L, Ahrens B (2018) Mistral and Tramontane wind speed and wind direction patterns in regional climate simulations. *Clim Dyn* 51(3):1059–1076. <https://doi.org/10.1007/s00382-016-3053-3>
- Oki T, Sud YC (1998) Design of total runoff integrating pathways (TRIP)—a global river channel network. *Earth Interact* 2(1):1–37. [https://doi.org/10.1175/1087-3562\(1998\)002<0001:DOTRIP>2.3.CO;2-oki-1998](https://doi.org/10.1175/1087-3562(1998)002<0001:DOTRIP>2.3.CO;2-oki-1998)
- Pfahl S, Schwierz C, Croci-Maspoli M, Grams CM, Wernli H (2015) Importance of latent heat release in ascending air streams for atmospheric blocking. *Nat Geosci* 8(8):610–614. <https://doi.org/10.1038/ngeo2487>
- Poli P, Hersbach H, Dee DP, Berrisford P, Simmons AJ, Vitart F, Laloyaux P, Tan DGH, Peubey C, Thépaut JN, Trémolet Y, Hólm EV, Bonavita M, Isaksen L, Fisher M (2016) ERA-20C: an atmospheric reanalysis of the twentieth century. *J Clim* 29(11):4083–4097. <https://doi.org/10.1175/JCLI-D-15-0556.1>
- Primo C, Kelemen FD, Feldmann H, Akhtar N, Ahrens B (2019) A regional atmosphere-ocean climate system model (CCLMv5.0clm7-NEMOv3.3-NEMOv3.6) over Europe including three marginal seas: on its stability and performance. *Geosci Model Dev* 12(12):5077–5095. <https://doi.org/10.5194/gmd-12-5077-2019>
- R Core Team (2013) R: a language and environment for statistical computing. R Foundation for Statistical Computing, Vienna, Austria. <http://www.R-project.org/>, ISBN 3-900051-07-0. Accessed 10 Dec 2020
- Rockel B, Will A, Hense A (2008) The Regional Climate Model COSMO-CLM (CCLM). *Meteorol Z* 17(4):347–348. <https://doi.org/10.1127/0941-2948/2008/0309>
- Schär C, Lüthi D, Beyerle U, Heise E (1999) The soil-precipitation feedback: a process study with a regional climate model. *J Clim* 12(3):722–741. [https://doi.org/10.1175/1520-0442\(1999\)012<0722:TSPFAP>2.0.CO;2](https://doi.org/10.1175/1520-0442(1999)012<0722:TSPFAP>2.0.CO;2)
- Schröter K, Kunz M, Elmer F, Mühr B, Merz B (2015) What made the June 2013 flood in Germany an exceptional event? A hydro-meteorological evaluation. *Hydrol Earth Syst Sci* 19(1):309–327. <https://doi.org/10.5194/hess-19-309-2015>
- Schulzweida U (2021) Cdo user guide. <https://doi.org/10.5281/zenodo.5614769>

- Sevaut F, Somot S, Alias A, Dubois C, Lebeau-pin-Brossier C, Nabat P, Adloff F, Déqué M, Decharme B (2014) A fully coupled Mediterranean regional climate system model: design and evaluation of the ocean component for the 1980–2012 period. *Tellus A Dyn Meteorol Oceanogr* 66(1):23967. <https://doi.org/10.3402/tellusa.v66.23967>
- Sodemann H, Zubler E (2010) Seasonal and inter-annual variability of the moisture sources for Alpine precipitation during 1995–2002. *Int J Climatol*. <https://doi.org/10.1002/joc.1932>
- Sodemann H, Schwierz C, Wernli H (2008) Interannual variability of Greenland winter precipitation sources: Lagrangian moisture diagnostic and North Atlantic Oscillation influence. *J Geophys Res* 113(D3):D03107. <https://doi.org/10.1029/2007JD008503>
- Sodemann H, Wernli H, Schwierz C (2009) Sources of water vapour contributing to the Elbe flood in August 2002—A tagging study in a mesoscale model. *Q J R Meteorol Soc* 135(638):205–223. <https://doi.org/10.1002/qj.374>
- Sorg W (1926) Ursachen und Verlauf des Oder-Hochwassers vom Juni 1926. *Geographischer Anzeiger* 27:262–265 (**gotha**)
- Spearman C (1904) The proof and measurement of association between two things. *Am J Psychol* 15(1):72. <https://doi.org/10.2307/1412159>, <https://www.jstor.org/stable/1412159?origin=crossref>
- Sprengrer M, Wernli H (2015) The LAGRANTO Lagrangian analysis tool—version 2.0. *Geosci Model Dev* 8(8):2569–2586. <https://doi.org/10.5194/gmd-8-2569-2015>
- Sprengrer M, Fragkoulidis G, Binder H, Croci-Maspoli M, Graf P, Grams CM, Knippertz P, Madonna E, Schemm S, Škerlak B, Wernli H (2017) Global climatologies of Eulerian and Lagrangian flow features based on ERA-Interim. *Bull Am Meteorol Soc* 98(8):1739–1748. <https://doi.org/10.1175/BAMS-D-15-00299.1>
- Stahl N, Hofstätter M (2018) Vb-Zugbahnen und deren Auftreten als Serie mit Bezug zu den resultierenden Hochwassern in Bayern und Auswirkungen auf Rückhalteräume im Isareinzugsgebiet. *Hydrol Wasserbewirtsch* 62(2):77–97. [https://doi.org/10.5675/HyWa\\_2018,2\\_2](https://doi.org/10.5675/HyWa_2018,2_2)
- Steinfeld D, Pfahl S (2019) The role of latent heating in atmospheric blocking dynamics: a global climatology. *Clim Dyn* 53(9–10):6159–6180. <https://doi.org/10.1007/s00382-019-04919-6>
- Steinfeld D, Boettcher M, Forbes R, Pfahl S (2020) The sensitivity of atmospheric blocking to upstream latent heating—numerical experiments. *Weather Clim Dyn* 1(2):405–426. <https://doi.org/10.5194/wcd-1-405-2020>
- Tarasova L, Merz R, Kiss A, Basso S, Blöschl G, Merz B, Viglione A, Plötner S, Guse B, Schumann A, Fischer S, Ahrens B, Anwar F, Bárdossy A, Bühler P, Haberlandt U, Kreibich H, Krug A, Lun D, Müller-Thomy H, Pidoto R, Primo C, Seidel J, Vorogushyn S, Wietzke L (2019) Causative classification of river flood events. *Wiley Interdiscip Rev Water* 6(4):e1353. <https://doi.org/10.1002/wat2.1353>
- Trigo IF, Bigg GR, Davies TD (2002) Climatology of cyclogenesis mechanisms in the Mediterranean. *Mon Weather Rev* 130(3):549–569. [https://doi.org/10.1175/1520-0493\(2002\)130%3c0549:COCMIT%3e2.0.CO;2](https://doi.org/10.1175/1520-0493(2002)130%3c0549:COCMIT%3e2.0.CO;2)
- Uhlemann S, Thieken A, Merz B (2010) A consistent set of trans-basin floods in Germany between 1952–2002. *Hydrol Earth Syst Sci* 14(7):1277–1295. <https://doi.org/10.5194/hess-14-1277-2010>
- Ulbrich U, Brücher T, Fink AH, Leckebusch GC, Krüger A, Pinto JG (2003a) The central European floods of August 2002: part 1—rainfall periods and flood development. *Weather* 58(10):371–377. <https://doi.org/10.1256/wea.61.03A>
- Ulbrich U, Brücher T, Fink AH, Leckebusch GC, Krüger A, Pinto JG (2003b) The central European floods of August 2002: Part 2—synoptic causes and considerations with respect to climatic change. *Weather* 58(11):434–442. <https://doi.org/10.1256/wea.61.03B>
- van Beber WJ (1891) Die Zugstrassen der barometrischen Minima nach den Bahnenkarten der deutschen Seewarte für den Zeitraum 1875–1890. *Meteorol Z* 8:361–366
- Volosciuk C, Maraun D, Semenov VA, Tilinina N, Gulev SK, Latif M (2016) Rising Mediterranean Sea surface temperatures amplify extreme summer precipitation in Central Europe. *Sci Rep* 6(1):32450. <https://doi.org/10.1038/srep32450>
- Weichmann (1931) Der Hochwasserschutz in Schlesien und die Lehrendes Hochwassers vom Herbst 1930. *Der Kulturtechniker* 34(3/4):258–272 (**breslau**)
- Wernli H, Davies HC (1997) A Lagrangian-based analysis of extratropical cyclones. I: the method and some applications. *Q J R Meteorol Soc* 123(538):467–489. <https://doi.org/10.1256/smsqj.53810>
- Wernli H, Schwierz C (2006) Surface cyclones in the ERA-40 Dataset (1958–2001). Part I: novel identification method and global climatology. *J Atmos Sci* 63(10):2486–2507. <https://doi.org/10.1175/JAS3766.1>
- Wenschall A (2013) Evaporative moisture sources for heavy precipitation events. PhD thesis, ETH Zurich, <https://doi.org/10.3929/ethz-a-009755505>
- Wenschall A, Pfahl S, Sodemann H, Wernli H (2014) Comparison of Eulerian and Lagrangian moisture source diagnostics—the flood event in eastern Europe in May 2010. *Atmos Chem Phys* 14(13):6605–6619. <https://doi.org/10.5194/acp-14-6605-2014>

**Publisher's Note** Springer Nature remains neutral with regard to jurisdictional claims in published maps and institutional affiliations.